In vitro assessments of reverse glenoid stability using displacement gages are misleading - recommendations for accurate measurements of interface micromotion

Favre, P ; Perala, S ; Vogel, P ; Fucentese, S F ; Goff, J R ; Gerber, C ; Snedeker, J G

Abstract: BACKGROUND: Baseplate micromotion of the reverse shoulder glenoid component can lead to implant loosening. We hypothesized that a remotely positioned displacement gage measures elastic deformation of the system rather than actual micromotion at the implant/bone interface. METHODS: Reverse glenoid components were implanted into polyurethane blocks of 3 different densities. A 700 N compressive load was maintained and a vertical 700 N shear load was applied for 1000 cycles. In addition to the typical gage measurement, a digital image analysis of micromotion at the implant/block interface using high resolution cameras was performed. The measurements were validated on human specimens. A finite element model was implemented to study the isolated effect of block deformation on baseplate displacements. FINDINGS: With the gage, typically reported micromotions were measured. Two orders of magnitude lower micromotions were detected using interface image-based analysis. The finite element simulation showed that elastic deformation alone can cause micromotion magnitudes as measured with displacement gages. Polyurethane blocks of 20 and 15 lbs per cubic foot density best reproduced micromotions as measured on human specimens. INTERPRETATION: We found considerably less relative micromotion at the implant/bone interface than previously assumed. Gage measurements quantify elastic deformation and not true interface micromotion. High resolution digital imaging at the implant/bone interface is strongly recommended for an accurate assessment of reverse glenoid component micromotion. Tests should further adopt 20 or 15 pcf bone test surrogates. Further studies are required to identify the failure modes encountered in vivo, and a corresponding in vitro testing methodology can then be developed.

DOI: https://doi.org/10.1016/j.clinbiomech.2011.05.002

IN VITRO ASSESSMENTS OF REVERSE GLENOID STABILITY USING DISPLACEMENT GAGES ARE MISLEADING– Recommendations for accurate measurements of interface micromotion

Philippe Favre, MSc*, Scott Perala, MSc, Peter Vogel, MSc, Sandro F. Fucentese, MD, Jonathan R. Goff, MD, Christian Gerber, MD, Jess G. Snedeker, PhD

Laboratory for Orthopedic Research, Department of Orthopedics, Balgrist, University of Zurich, Switzerland

*Corresponding author

Forchstrasse 340

8008 Zurich, Switzerland

Tel.: +41 44 386 1672

Fax: +41 44 386 1109

E-mail: pfavre@research.balgrist.ch

ABSTRACT

Background: Baseplate micromotion of the reverse shoulder glenoid components can lead to implant loosening. We hypothesized that a remotely positioned displacement gage measures elastic deformation of the system rather than actual micromotion at the implant/bone interface.

Methods: Reverse glenoid components were implanted into polyurethane blocks of 3 different densities. A 700N compressive load was maintained and a vertical 700N shear load was applied for 1'000 cycles. In addition to the typical gage measurement, a digital image analysis of micromotion at the implant/block interface using high resolution cameras was performed. The measurements were validated on human specimens. A finite element model was implemented to study the isolated effect of block deformation on baseplate displacements.

Findings: With the gage, typically reported micromotions were measured. Two orders of magnitude lower micromotions were detected using interface image-based analysis. The finite element simulation showed that elastic deformation alone can cause micromotion magnitudes as measured with displacement gages. Polyurethane blocks of 20 and 15 pounds per cubic foot density best reproduced micromotions as measured on human specimens.

Interpretation: We found considerably less relative micromotion at the implant/bone interface than previously assumed. Gage measurements quantify elastic deformation and not true interface micromotion. High resolution digital imaging at the implant/bone interface is strongly recommended for an accurate assessment of reverse glenoid

component micromotion. Tests should further adopt 20 or 15 pcf bone test surrogates. Further studies are required to identify the failure modes encountered in vivo, and a corresponding in vitro testing methodology can then be developed.

Keywords: Micromotion, glenoid loosening, implant testing, reverse shoulder arthroplasty/replacement, reverse/delta prosthesis, high resolution image analysis, displacement gage.

INTRODUCTION

Reverse total shoulder arthroplasty has been shown to improve function and pain in the treatment of massive rotator cuff tear and cuff tear arthropathy, rheumatoid arthritis, fractures, or revision arthroplasty (Boileau et al., 2006, Gerber et al., 2009, Guery et al., 2006, Sirveaux et al., 2004, Werner et al., 2005). Nevertheless, the rate of problems remains high, in part because of glenoid component loosening (Gerber et al., 2009, Mole and Favard, 2007). Micromotion from 28 to 150 micrometers (µm) has been shown to inhibit bone ingrowth and lead to an unstable fibrous tissue layer between a metallic implant and the host bone (Cameron et al., 1973, Ducheyne et al., 1977, Jasty et al., 1997a, Jasty et al., 1997b, Pilliar et al., 1986). Therefore, minimizing micromotion at the time of initial fixation should lead to better ingrowth of bone and a more stable implant. The current best practice for testing implant primary stability consists of measuring absolute micromotion of the reverse glenoid baseplate after cyclical loading by means of a displacement gage (DG) (Gutierrez et al., 2007, Harman et al., 2005, Kwon et al., 2010, Poon et al., 2010, Virani et al., 2008). These studies reported micromotions up to 100µm. The DG tip was placed on the baseplate alone, measuring the displacement of the gage relative to the frame on which the DG is fixed (up to 3 mm away from the bone/baseplate interface (Virani et al., 2008)). However, the cells responsible for bone ingrowth sense the relative motion of the baseplate at the interface to the bone. It is logical to assume that a more appropriate measurement method would therefore assess the micromotion of the baseplate relative to the bone, at the interface where osteointegration is required, rather than the absolute baseplate motion alone.

We first hypothesized that current remote DG measurements include deformation of the Sawbones and may not be representative of relative micromotion at the bone/implant interface. In order to test this hypothesis, quantification of micromotion with DG was compared against high resolution imaging (HRI) of the interface, and the deformation within the entire system was assessed using the finite element (FE) method. Second, while there currently exists no standard for assessing reverse glenoid component stability, the ASTM recommends using polyurethane blocks of modulus and strength corresponding to a density 20 pcf (pounds per cubic foot) for experimental testing of conventional and cemented glenoid component (ASTM, 2008). This density has been used in a few studies for the uncemented reverse glenoid component (Codsi and Iannotti, 2008, Poon et al., 2010), while a number of investigations implemented higher (Gutierrez et al., 2007, Harman et al., 2005, Virani et al., 2008) or lower density blocks (Chebli et al., 2008). Therefore, we hypothesized that the choice of the appropriate polyurethane bone test surrogates could be optimized to provide more relevant measurements of reverse glenoid micromotion. This was tested by comparing the micromotion on different densities of Sawbones blocks against measurements on human scapulae.

METHODS

Two measurement systems were compared: the DG (TESA SA, Renens, Switzerland; resolution of 10 μm), and a high resolution digital camera (Basler A622F, Basler Vision Technologies AG, Ahrensburg, Germany; pixel resolution of 6.70 μm) mounted with a 1x magnification telecentric lens (Zeiss Visionmes, Carl Zeiss AG, Jena, Germany).

The accuracy of the DG and the HRI methods was first assessed by measuring known levels of displacement imposed at the actuator of a universal testing machine with better than 1μm positional precision (Zwick 1456, Zwick GmbH&Co. KG, Ulm, Germany) (Codsi and Iannotti, 2008, Lee et al., 1998).

In vitro quantification of baseplate micromotion was then performed according to previously described studies (Figure 1) (Harman et al., 2005, Virani et al., 2008). Glenoid components of a Delta III™ reverse prosthesis (Depuy Orthopaedics, Inc. Warsaw, IN) were implanted according to manufacturer guidelines into polyurethane blocks (Sawbones, Malmö, Sweden) of 30 pcf density (Gutierrez et al., 2007, Harman et al., 2005). The baseplate was fixed with four 4.5mm diameter screws (Figure 1). A 30 mm long locking screw was used in the superior hole and oriented superiorly with a 17° angle relative to the peg axis. A 48 mm long locking screw was used in the inferior hole oriented inferiorly with a 17° angle relative to the peg axis. A 36 mm cortical screw was inserted in the anterior hole and an 18 mm screw was placed in the posterior hole, both oriented parallel to the peg axis. Drill guides were used to obtain the recommended angles. In order to permit visual access to the interface between the baseplate and the glenoid for the HRI, two modifications were performed (Figure 1). First, prior to fixation

of the glenosphere to the baseplate, a small portion of the glenosphere was milled out (Codsi and Iannotti, 2008). Second, the Sawbones block was milled on the imaging side until reaching the protrusion created by the manufacturer tooling (glenoid rasp).

The setup holding the polyurethane block was fixed on two orthogonally mounted linear tables (SFERAX SA, Cortaillod, Switzerland) to simulate the anterior-posterior and medio-lateral translational degrees of freedom of the shoulder joint (Favre et al., 2010). The block was placed on a horizontal metal plate and a constant 700N compressive load was applied between the polyethylene component and glenosphere from medial to lateral by means of static weights and pulleys attached to the corresponding linear table. This pressed the block on the medial side against a vertical metal plate, to which a third metal plate was then screwed to secure the block in the inferior-superior direction. In this manner, the block was rigidly constrained and no motion relative to the holding frame was allowed.

The starting position of the components was defined as fully centered. The glenoid component being able to freely translate in the anterior-posterior and medio-lateral directions by virtue of the two linear tables, the components were automatically centered along these directions by the compressive load. To center the components in the remaining direction, a minimum inferior-superior load was searched with the testing machine. From this starting position, a shear force of 700 N was then cyclically applied in the inferior and superior directions through translations of the polyethylene component at a rate of 300N/s for 1’000 cycles.

For validation purposes, two Thiel preserved (Thiel, 1992), left-side, human scapulae were tested using the same testing and measurement protocol as for the Sawbones. No donor information was available, but the bones were verified to be free of any visible pathologies. The medial half of the scapula, the coracoid process and the acromion were cut away to allow fixation of the specimen (Hoenig et al., 2009, Kwon et al., 2010). The remaining medial portion of the bone was potted (Codsi and Iannotti, 2008, Hoenig et al., 2009, Kwon et al., 2010) in an epoxy resin cylinder (Struers A/S, Ballerup, Denmark) to obtain a secure fixation of the bone to the set up while simultaneously isolating the bone from deformations induced by the clamps. The cylinder was finally fixed to the testing machine with a custom clamping system with radially oriented screws (Supplementary data Figure 1). Micromotion testing was then performed in a strictly identical manner to the Sawbones testing.

Micromotion was measured with the DG, placing the measuring tip against the most inferior aspect of the baseplate and as close as possible to the baseplate-foam interface, reproducing methods described in the literature (Harman et al., 2005, Poon et al., 2010, Virani et al., 2008). In order to access the baseplate with the DG measuring tip, the milled portion of the glenosphere created for HRI was positioned inferiorly. In addition a HRI analysis of micromotion at the implant/block interface was performed (Codsi and Iannotti, 2008), before and after the 1'000 cycles. The imaging axis of the lens was kept perpendicular to the analyzed border at the implant/block interface. A first digital image of the Sawbones/baseplate interface was captured with 700 N of compressive force only and a second image was captured with a superimposed load of

700 N shear force applied in a vertical direction. Micromotion at the interface of the implant baseplate and the sawbone block was computed using in-house written code combining Matlab (The MathWorks, Natick, MA, USA) and ImageJ (http://rsb.info.nih.gov/ij/). The ImageJ plugin SIFT (Lowe, 2004) was implemented to automatically identify as many sets of corresponding points as possible in the two images within 0.5 mm on both sides of the interface over a 2mm inferior-superior height. A common reference system was defined for both images to remove any rotation and translation of the system or the camera. To do so, the baseplate was considered as a rigid body and rotation and translation matrices were defined in order to overlap the baseplate points on both images. In this configuration, the baseplate could be considered as a fixed reference and the change in position of points on the Sawbones between the two images corresponded to the micromotion. The difference was converted from pixels to μm using calibration images of known dimensions, and served as the quantification of micromotion at the interface of the baseplate and the Sawbones foam (shown by the blue arrows on the close-up of Figure 1). Micromotion for all landmarks within the region of interest was finally averaged. This was repeated for three different locations of the interface; one centered at the middle of the inferior-superior height of the baseplate, and one each at the height of the intersections of the inferior and superior screws with the baseplate (Figure 1). HRI results report the total two dimensional micromotion (resultant of the inferior-superior and medio-lateral components). When comparing against the uniaxial DG measurements of the 30 pcf blocks, only the vertical component of HRI micromotion was considered.

DG measurements were performed on the 30 pcf blocks only. Using HRI, 15, 20 and 30 pcf Sawbones blocks were tested to assess the influence of block rigidity on true micromotion.

Three samples per Sawbones block density were prepared (Harman et al., 2005). An unpaired Students t-test was used, except for the pre/post-cycle comparison where a paired t-test was performed. Statistical significance was set to $P<0.05$.

Finally, a three-dimensional FE model was built to reproduce the experimental setup and assess the isolated influence of block deformation on baseplate displacement at the location of DG measurement. The implant and polyurethane block geometries were created by physical inspection and the screws were modeled as cylinders with a diameter of 4.5mm (Hopkins and Hansen, 2009, Hopkins et al., 2008, Virani et al., 2008). The prosthesis was implanted virtually in the block as in the experiments. After mesh convergence analysis, the model was meshed with a total of 77'000 quadratic tetrahedral elements in ANSYS 12.0 Workbench (Ansys Inc., Canonsburg, PA, USA). Linear isotropic material properties of titanium (Elastic modulus=96GPa, Poisson's ratio=0.36) were assigned to the baseplate and screws, cobalt-chrome (Elastic modulus =200GPa, Poisson's ratio=0.3) to the glenosphere, and to the Sawbones blocks according to the manufacturer (Elastic modulus of 150, 250, 500 GPa to the 15, 20, 30 pcf respectively and Poisson's ratio of 0.24 for all). The block was fixed in rotation and translation at the top, bottom, and back sides to prevent any possible shift of the block. Fully bonded contacts were defined between all parts of the model in order to prevent any relative motion and isolate the influence of the block deformation on the

displacements. Superimposed static 700N compressive and 700N shear loads were applied on the glenosphere.

RESULTS

Both measurement systems, DG and HRI, achieved similar measurement precision and could accurately capture micromotion in a range of 0 to 80µm (Supplementary data Figure 2).

DG measurements on 30 pcf Sawbones registered displacement data in the same order of magnitude to that reported in similar studies (Table 1) (Harman et al., 2005, Virani et al., 2008). In contrast, HRI analysis of the interface resulted in much lower values.

No statistical difference was detected before and after 1'000 cycles for any of the investigated Sawbones densities at the inferior (P=0.94 for 30pcf, P=0.10 for 20pcf, P=0.47 for 15pcf), middle (P=0.68 for 30pcf, P=0.66 for 20pcf, P=0.71 for 15pcf), and superior (P=0.35 for 30pcf, P=0.81 for 20pcf, P=0.71 for 15pcf) imaging locations (Figure 2). Micromotion in the medio-lateral direction amounted in average 26% for the 30 pcf, 19% for the 20 pcf and up to 30% for the 15pcf of the total 2D micromotion.

The micromotion obtained with 15 and 20 pcf Sawbones samples overlapped in the inferior and superior measurement locations with the corridor defined by the measurements performed on the human scapulae (Supplementary Figure 3). For the middle location, the 15 and 20 pcf Sawbones were very close to the human scapula data. The micromotions quantified on 30 pcf blocks were all lower than the micromotions on human bones.

The strain distribution obtained from the FE simulation demonstrated that system deformation was present in the Sawbones (Figure 3). Elastic deformation of the foam alone led to apparent baseplate displacements at the DG measurement location in the

order of magnitude typically monitored by the DG (Table 2). Also, the displacements found in the block were directly related to the block density, with larger displacement occurring in blocks of lower density and elastic modulus (Table 2).

DISCUSSION

The long term success of reverse shoulder replacement relies on a secure primary fixation of the glenoid component. Reliable and accurate interface micromotion test methods are necessary in order to draw correct clinical conclusions regarding component positioning (Gutierrez et al., 2007), the choice of screw insertion angle, screw length, screw diameter (Hopkins et al, 2008), screw number (Hoening et al, 2009), or the sufficiency of an implant design (Poon et al, 2010, Hopkins et al, 2009, Kwon et al, 2010, Virani et al, 2008). This is also of paramount importance in numerical modelling studies that use such experimental data as baseline for validation (Hopkins and Hansen, 2009, Hopkins et al., 2008, Virani et al., 2008).

This study found that there was considerably less relative micromotion at the baseplate/bone interface than reported previously (Harman et al., 2005, Virani et al., 2008), even less than the lowest threshold of in vivo bone ingrowth inhibition (28μm), bone (Pilliar et al., 1986). The FE simulation revealed that elastic deformation of the Sawbones alone resulted in baseplate displacement inversely proportional to the Sawbones elastic modulus and of the order of magnitude typically reported by the experimental DG measurements. This demonstrates that a remotely positioned DG cannot differentiate the deformation of the Sawbones foam from micromotion at the interface. This artefact can be avoided with direct image-based analysis of relative motion at the implant/bone interface. Technically, HRI could also be applied to the testing of standard shoulder prostheses.

This study confirms the potential limitations of DG measurements or linear variable differential transducers to quantify micromotion that have been acknowledged by others (Anglin et al., 2000a, Bicknell et al., 2003, Collins et al., 1992, Karduna et al., 1998). The use of a single DG placed inferiorly on the glenosphere can only quantify vertical motion, and therefore any "Rocking Horse" effect is not detected (Anglin et al., 2000a, Anglin et al., 2000b, Franklin et al., 1988). Conversely, HRI analysis allows assessment of displacements in 2D (shear and rocking). Although micromotion of the reverse component occurs mainly in shear (Hoenig et al., 2009), we measured 1/5 to 1/3 of the total micromotion in the medio-lateral direction. This substantial contribution is neglected with a unidirectional measurement.

Comparison between studies is impaired by a current absence of standards for assessing reverse glenoid stability. A recent study implemented image analysis to assess micromotion of a reverse shoulder prosthesis (Codsi and Iannotti, 2008). Despite use of an imaging approach, micromotion levels up to 100 µm were reported for the standard implantation. Differences with our results may stem from several sources. The loading configuration was different with the humerus positioned at 20° abduction and with the implant loaded in the superior direction only. Scapula replicas instead of biomechanical testing blocks were used, achieving a less optimal (but possibly more realistic) screw purchase. Standard camera optics were used, which are sensitive to out of plane movements, in contrast to telecentric optics as implemented in the present study. The use of single point manual tracking at the interface may be less reliable than our fully automated multi-point tracking. Our own experiments using a similar set-up (Sawbones

scapulae implanted with identical prostheses and analyzed with HRI), yielded measurements of very little micro-motion (data not shown).

Conversely several studies reported micromotions obtained with a displacement gage that were closer to our HRI values (Gutierrez et al., 2007, Kwon et al., 2010, Poon et al., 2010). Comparison with these studies is difficult for several reasons. Different degrees of abduction were simulated, loads of varying directions were applied and the resultant magnitude was up to three times lower than the values used in the present study. In addition, the number of loading cycles varied from ten (Gutierrez et al., 2007), to 1'000 (Poon et al., 2010), to 10'000 (Kwon et al., 2010).

Displacement values reported by previous FE studies were generally lower than found in our FE model (Hopkins et al., 2008, Virani et al., 2008). This difference may stem from the implementation of frictional contacts between the block and the baseplate to simulate micromotion. A higher coefficient of friction has been shown to lead to larger displacements (Virani et al., 2008) and we considered ideally bonded contacts to segregate the effect of block deformation. Interestingly, relative interface micromotion was already indicated to differ from baseplate displacements with respect to a fixed frame of reference (Hopkins et al., 2008).

In vitro biomechanical testing studies of the reverse implant (Harman et al., 2005, Virani et al., 2008) were adapted from methods developed for conventional implant testing (Anglin et al., 2000a, Fukuda et al., 1988). However, major methodological divergences are present. In conventional implant testing, the rocking horse phenomenon was assessed by measuring the medio-lateral motion of the glenoid component after

100’000 cycles to reproduce a 25 years in vivo use. In reverse implant testing, the inferior-superior motion of the whole construct was measured, and this after only 1’000 cycles to model the immediate postoperative situation. The lack of micromotion in the reverse shoulder implants we observed may be due to less aggressive biomechanical loading or more robust fixation than has been reported for conventional total shoulder arthroplasty (Anglin et al., 2000a, Collins et al., 1992). On the other hand, our in vitro results may confirm clinical studies that rarely observed glenoid loosening in the initial postoperative period (Boileau et al., 2006, Werner et al., 2005). This would suggest that in vivo loosening of the reverse glenoid component may not be due to poor primary stability but could be attributed to other factors such as poor secondary stability due to inadequate bone quality, insufficient screw purchase or component malpositioning (Guery et al., 2006, Werner et al., 2005). If these are the failure modes, appropriate in vitro biomechanical test standards should be developed to address these particular clinical problems. In order to test if micromotion is a failure mode, more clinical studies are now required to establish whether a fibrous tissue layer has been found at the interface of failed reverse glenoid components. Also, valuable information could be obtained by comparing if particular implant models fail more often than others, and under which particular conditions.

Sawbones block density has been shown to directly affect the load to failure of glenoid component fixation (Chebli et al., 2008). The validation experiment indicated that Sawbones block density also had a notable effect on micromotion magnitude, with 15 and 20 pcf blocks more closely matching results from the tested human scapulae.

Sawbone blocks of 15 and 20 pcf density may be therefore preferable in assessing micromotion, confirming that the ASTM recommendations for conventional and cemented glenoid testing on polyurethane block density (ASTM, 2008) can be partly transferred to reverse and uncemented glenoid testing. Although relative differences may be large when comparing micromotions from blocks of different densities, absolute values of micromotion remained very low, especially when compared to previously reported values and to the limits needed to create loosening. In any case, caution should be exercised when equating micromotion measured on Sawbones with the physiological limits on bone ingrowth (Cameron et al., 1973, Ducheyne et al., 1977, Jasty et al., 1997a, Jasty et al., 1997b, Pilliar et al., 1986).

Limitations to the present study include that the Sawbones blocks and human scapulae were rigidly fixed (as in all previous studies of micromotion), which is not the case in vivo. No information was available on the bone donors and the bone quality was not assessed. As an in vitro model, Sawbones are also limited in that they provide uniform and consistent bone quality that is not representative of natural variety found in vivo. Nonetheless, the validation showed that the very low micromotions obtained with these surrogates are comparable to what was measured on human specimens. We only tested two human Thiel preserved scapulae. A larger number of fresh specimens of known gender, age and bone density should be tested in the future in order to draw more definitive conclusions on the selection of an appropriate Sawbones block density. Slightly lower compressive and shear loads than the standards for conventional cemented glenoids (ASTM, 2008) and previous studies (Harman et al., 2005, Virani et al.,

2008) were used. However, the same loading conditions were implemented for the DG and HRI measurements, warranting a direct comparison of the two techniques. While the joint reaction force was recently estimated in an analytical model for the reverse shoulder joint (Kwon et al., 2010) or measured in vivo for conventional shoulder implants (Westerhoff et al., 2009), a final limitation lies in the fact that the in vivo loads acting at the reverse shoulder joint still remain unknown, and are most likely different from the loading regimen applied in in vitro tests.

With regard to limitations on image-based assessment, HRI allows measuring micromotions in two dimensions (inferior-superior and medio-lateral), but cannot assess the anterior-posterior component. However, a three dimensional finite element model investigation of interface micromotion (manuscript in preparation) has indicated that micromotion in the anterior-posterior direction is one order of magnitude smaller than the other two components, and can likely be neglected.

The main limitation of the FE model was the ideally bonded contact representation at the block-screw and block-implant. However, this simplification was intentional to isolate the effect of the Sawbones deformation and discard any influence from implant disassembly or any large tilting of the glenosphere relative to the block that may occur during the experiments. While we did not observe such visible motions by eye, they may also account for a portion of the rather high experimental DG measurements we obtained. Static rather than cyclic loads were implemented in the FE model (Hopkins and Hansen, 2009, Hopkins et al., 2008). However, 1’000 loading cycles where shown to

have no influence on neither the displacement measured with DG (Virani et al., 2008) nor on our own HRI micromotion measurements (Figure 2).

CONCLUSIONS

We found considerably less relative micromotion at the interface between the reverse glenoid component baseplate and the scapula than previously reported. DG measurements quantify elastic deformation of the Sawbones material rather than true interface micromotion. High resolution digital imaging of the interface is strongly recommended for an accurate assessment of reverse glenoid component micromotion. Further, the selection of an appropriate bone test surrogate is key to an accurate assessment of implant stability, and using Sawbones blocks of 15 and 20pcf may be the preferred choice with respect to their ability to mimic micromotions measured in vitro using actual human scapulae. Further work needs to be done to develop an appropriate in vitro testing methodology that corresponds to the failure modes encountered in vivo.

ACKNOWLEDGMENTS:

The authors acknowledge the technical assistance given by Mr. H.R. Sommer of the department of orthopaedics, Balgrist, University of Zurich. This was an internally financed study.

REFERENCES

Anglin, C., Wyss, U. P., Pichora, D. R., 2000a. Mechanical testing of shoulder prostheses and recommendations for glenoid design. J Shoulder Elbow Surg. 9, 323-31.

Anglin, C., Wyss, U. P., Pichora, D. R., 2000b. Shoulder prosthesis subluxation: theory and experiment. J Shoulder Elbow Surg. 9, 104-14.

Astm, 2008. F2028-08, Standard Test Methods for Dynamic Evaluation of Glenoid Loosening or Disassociation. American Society for Testing and Materials, West Conshohocken, PA.

Bicknell, R. T., Liew, A. S., Danter, M. R., Patterson, S. D., King, G. J., Chess, D. G., et al., 2003. Does keel size, the use of screws, and the use of bone cement affect fixation of a metal glenoid implant? J Shoulder Elbow Surg. 12, 268-75.

Boileau, P., Watkinson, D., Hatzidakis, A. M., Hovorka, I., 2006. Neer Award 2005: The Grammont reverse shoulder prosthesis: results in cuff tear arthritis, fracture sequelae, and revision arthroplasty. J Shoulder Elbow Surg. 15, 527-40.

Cameron, H. U., Pilliar, R. M., Macnab, I., 1973. The effect of movement on the bonding of porous metal to bone. J Biomed Mater Res. 7, 301-11.

Chebli, C., Huber, P., Watling, J., Bertelsen, A., Bicknell, R. T., Matsen, F., 3rd, 2008. Factors affecting fixation of the glenoid component of a reverse total shoulder prothesis. J Shoulder Elbow Surg. 17, 323-7.

Codsi, M. J., Iannotti, J. P., 2008. The effect of screw position on the initial fixation of a reverse total shoulder prosthesis in a glenoid with a cavitary bone defect. J Shoulder Elbow Surg. 17, 479-86.

Collins, D., Tencer, A., Sidles, J., Matsen, F., 3rd, 1992. Edge displacement and deformation of glenoid components in response to eccentric loading. The effect of preparation of the glenoid bone. J Bone Joint Surg Am. 74, 501-7.

Ducheyne, P., De Meester, P., Aernoudt, E., 1977. Influence of a functional dynamic loading on bone ingrowth into surface pores of orthopedic implants. J Biomed Mater Res. 11, 811-38.

Favre, P., Sussmann, P. S., Gerber, C., 2010. The effect of component positioning on intrinsic stability of the reverse shoulder arthroplasty. J Shoulder Elbow Surg. 19, 550-6.

Franklin, J. L., Barrett, W. P., Jackins, S. E., Matsen, F. A., 3rd, 1988. Glenoid loosening in total shoulder arthroplasty. Association with rotator cuff deficiency. J Arthroplasty. 3, 39-46.

Fukuda, K., Chen, C. M., Cofield, R. H., Chao, E. Y., 1988. Biomechanical analysis of stability and fixation strength of total shoulder prostheses. Orthopedics. 11, 141-9.

Gerber, C., Pennington, S. D., Nyffeler, R. W., 2009. Reverse total shoulder arthroplasty. J Am Acad Orthop Surg. 17, 284-95.

Guery, J., Favard, L., Sirveaux, F., Oudet, D., Mole, D., Walch, G., 2006. Reverse total shoulder arthroplasty. Survivorship analysis of eighty replacements followed for five to ten years. J Bone Joint Surg Am. 88, 1742-7.

Gutierrez, S., Greiwe, R. M., Frankle, M. A., Siegal, S., Lee, W. E., 3rd, 2007. Biomechanical comparison of component position and hardware failure in the reverse shoulder prosthesis. J Shoulder Elbow Surg. 16, S9-S12.

Harman, M., Frankle, M., Vasey, M., Banks, S., 2005. Initial glenoid component fixation in reverse total shoulder arthroplasty: a biomechanical evaluation. J Shoulder Elbow Surg. 14, 162S-167S.

Hoenig, M. P., Loeffler, B., Brown, S., Peindl, R., Fleischli, J., Connor, P., et al., 2009. Reverse glenoid component fixation: is a posterior screw necessary? J Shoulder Elbow Surg. 19, 544-9.

Hopkins, A. R., Hansen, U. N., 2009. Primary stability in reversed-anatomy glenoid components. Proc Inst Mech Eng H. 223, 805-12.

Hopkins, A. R., Hansen, U. N., Bull, A. M., Emery, R., Amis, A. A., 2008. Fixation of the reversed shoulder prosthesis. J Shoulder Elbow Surg. 17, 974-80.

Jasty, M., Bragdon, C., Burke, D., O'connor, D., Lowenstein, J., Harris, W. H., 1997a. In vivo skeletal responses to porous-surfaced implants subjected to small induced motions. J Bone Joint Surg Am. 79, 707-14.

Jasty, M., Bragdon, C. R., Zalenski, E., O'connor, D., Page, A., Harris, W. H., 1997b. Enhanced stability of uncemented canine femoral components by bone ingrowth into the porous coatings. J Arthroplasty. 12, 106-13.

Karduna, A. R., Williams, G. R., Iannotti, J. P., Williams, J. L., 1998. Total shoulder arthroplasty biomechanics: a study of the forces and strains at the glenoid component. J Biomech Eng. 120, 92-9.

Kwon, Y. W., Forman, R. E., Walker, P. S., Zuckerman, J. D., 2010. Analysis of reverse total shoulder joint forces and glenoid fixation. Bull NYU Hosp Jt Dis. 68, 273-80.

Lee, T. Q., Danto, M. I., Kim, W. C., 1998. Initial stability comparison of modular hip implants in synthetic femurs. Orthopedics. 21, 885-8.

Lowe, D. G., 2004. Distinctive image features from scale-invariant keypoints. International Journal of Computer Vision. 60, 91-110.

Mole, D., Favard, L., 2007. [Excentered scapulohumeral osteoarthritis]. Rev Chir Orthop Reparatrice Appar Mot. 93, 37-94.

Pilliar, R. M., Lee, J. M., Maniatopoulos, C., 1986. Observations on the effect of movement on bone ingrowth into porous-surfaced implants. Clin Orthop Relat Res. 108-13.

Poon, P. C., Chou, J., Young, D., Malak, S. F., Anderson, I. A., 2010. Biomechanical evaluation of different designs of glenospheres in the SMR reverse total shoulder prosthesis: micromotion of the baseplate and risk of loosening. Shoulder & Elbow. 2 94-99.

Sirveaux, F., Favard, L., Oudet, D., Huquet, D., Walch, G., Mole, D., 2004. Grammont inverted total shoulder arthroplasty in the treatment of glenohumeral osteoarthritis

with massive rupture of the cuff. Results of a multicentre study of 80 shoulders. J Bone Joint Surg Br. 86, 388-95.

Thiel, W., 1992. [The preservation of the whole corpse with natural color]. Ann Anat. 174, 185-95.

Virani, N. A., Harman, M., Li, K., Levy, J., Pupello, D. R., Frankle, M. A., 2008. In vitro and finite element analysis of glenoid bone/baseplate interaction in the reverse shoulder design. J Shoulder Elbow Surg. 17, 509-21.

Werner, C. M., Steinmann, P. A., Gilbart, M., Gerber, C., 2005. Treatment of painful pseudoparesis due to irreparable rotator cuff dysfunction with the Delta III reverse-ball-and-socket total shoulder prosthesis. J Bone Joint Surg Am. 87, 1476-86.

Westerhoff, P., Graichen, F., Bender, A., Halder, A., Beier, A., Rohlmann, A., et al., 2009. In vivo measurement of shoulder joint loads during activities of daily living. J Biomech. 42, 1840-9.

FIGURE LEGENDS

Figure 1: Schematic of the experimental test set up. Cut-outs were made on the glenosphere and Sawbones block to gain visible access to the interface (red outlined close-up view). For DG measurements, the glenosphere cut-out was oriented inferiorly (not shown here), to allow placing the tip of the DG against the baseplate at the most inferior aspect of the baseplate-foam interface. The superior, middle and inferior HRI measurement windows were centered at the intersection of the screws (dashed white lines) with the baseplate. The blue close-up shows a typical high resolution image of the interface, with the computed 2D displacement vectors (shown enlarged here for visualization) of the Sawbones (right) with respect to the baseplate (left). The total relative micromotion was computed as the average of all vectors. The vertical bar represents 100 micrometers.

Figure 2: Micromotion (resultant magnitude of shear and compressive components) captured with HRI before and after the 1'000 cycles for the 15, 20 and 30 pcf Sawbones, at the inferior (Inf), middle (Mid) and superior (Sup) locations.

Figure 3

Strain distribution obtained from the three dimensional FE model. The strain distributions were the same for the 15, 20 and 30 pcf densities, we therefore report values normalized to the maximal strain (set to 100%). Absolute values are given in Table 2.

SUPPLEMENTARY DATA

Figure 1: Human scapula specimen potted in an epoxy resin cylinder, leaving the glenoid exposed for testing (A). The medial half of the scapula, the coracoid process and the acromion were cut away. Specimen fixed to the testing machine with a custom clamping system using radially oriented screws (B).

Figure 2: Comparison of HRI and DG measurement accuracy with respect to the reference displacement of the actuator end (black line). Equations of the linear regressions fitted to the measured data are given.

Figure 3: Micromotion on Sawbones of 15, 20 and 30 pcf density compared to human specimen (shaded areas) using HRI.

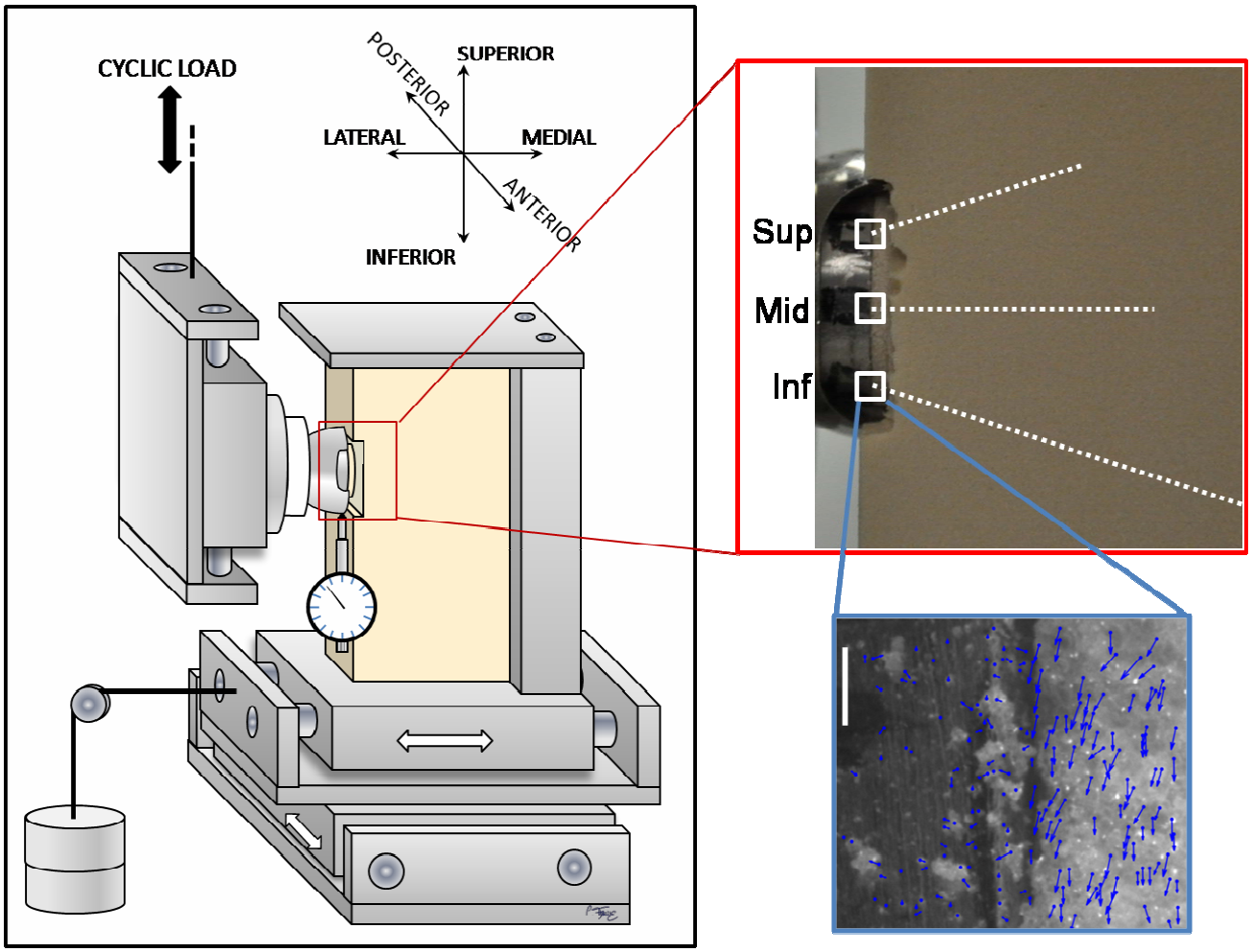
CYCLIC LOAD
POSTERIOR
SUPERIOR
LATERAL
MEDIAL
ANTERIOR
INFERIOR
Sup
Mid
Inf

Figure 1

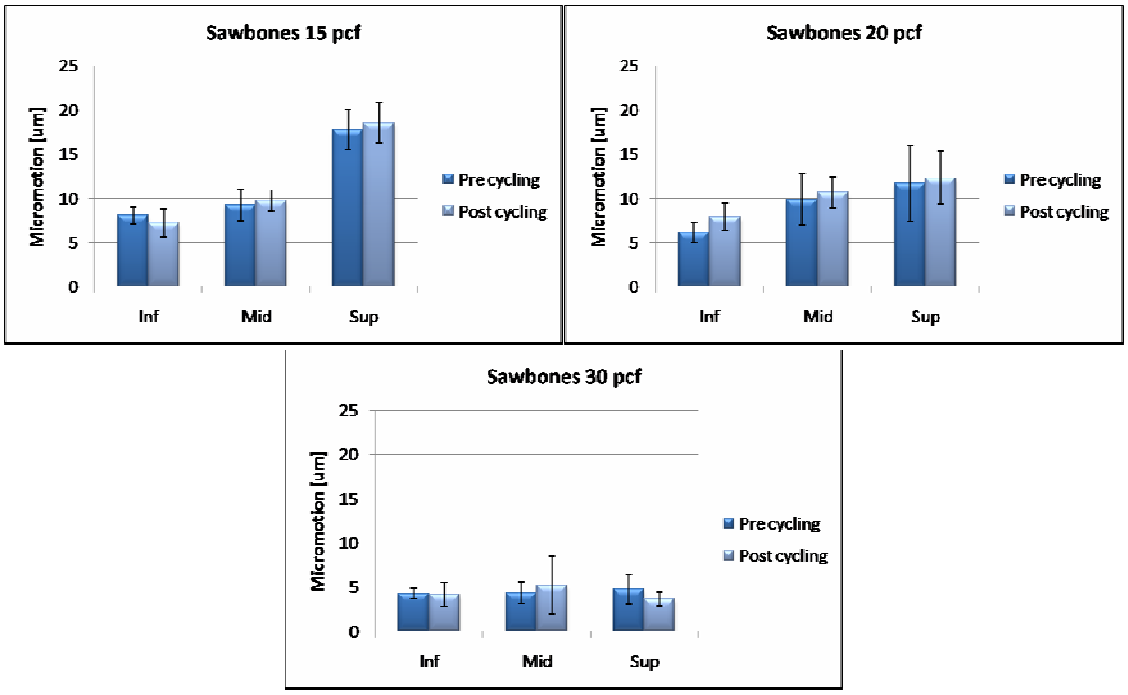
Sawbones 15 pcf
Micromotion [um]
25
20
15
10
5
0
Inf
Mid
Sup
Precycling
Post cycling
Sawbones 20 pcf
Micromotion [um]
25
20
15
10
5
0
Inf
Mid
Sup
Precycling
Post cycling
Sawbones 30 pcf
Micromotion [um]
25
20
15
10
5
0
Inf
Mid
Sup
Precycling
Post cycling

Figure 2

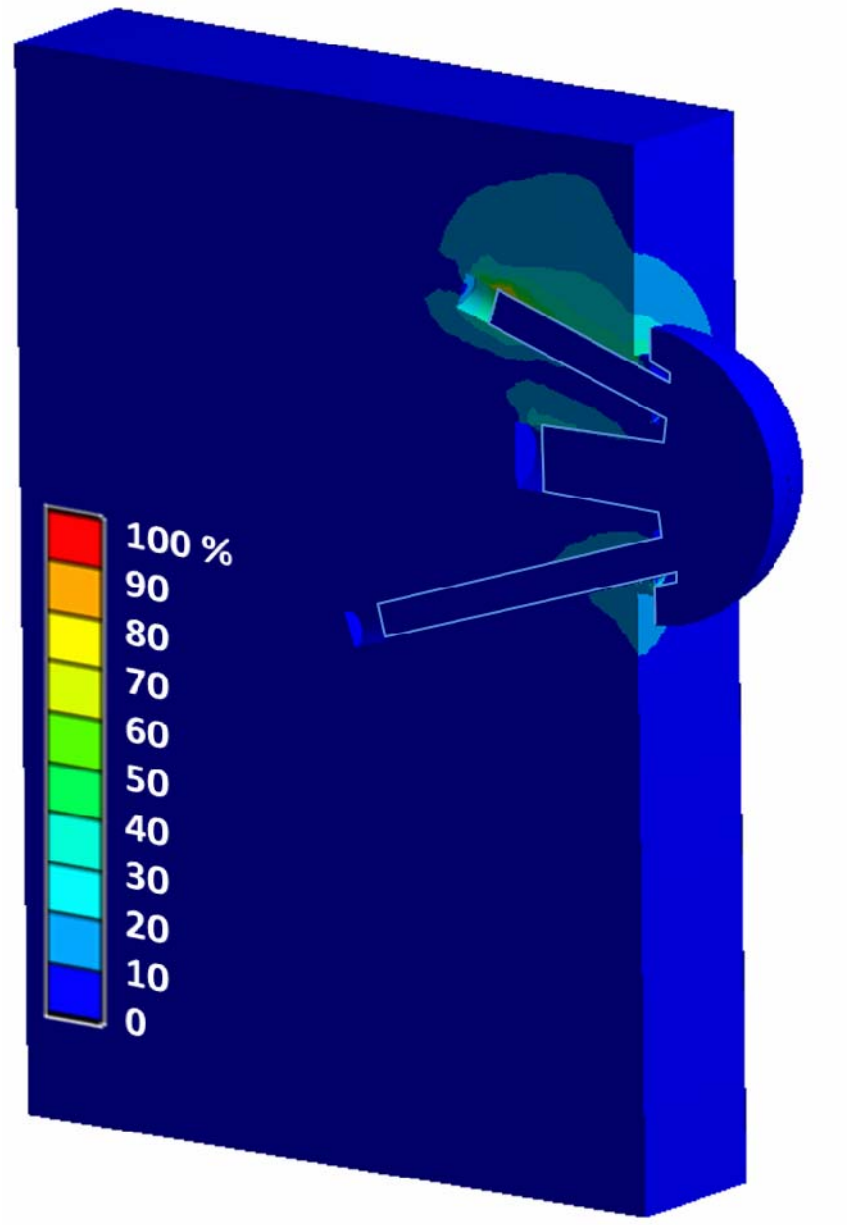

Figure 3

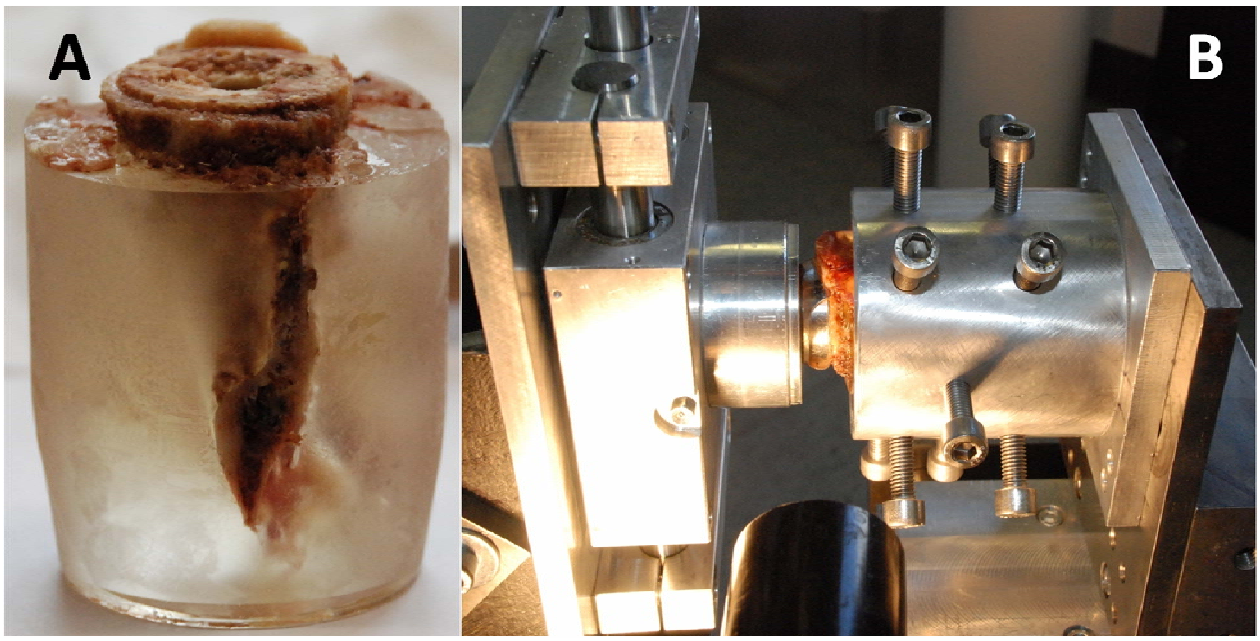

Supplementary Figure 1

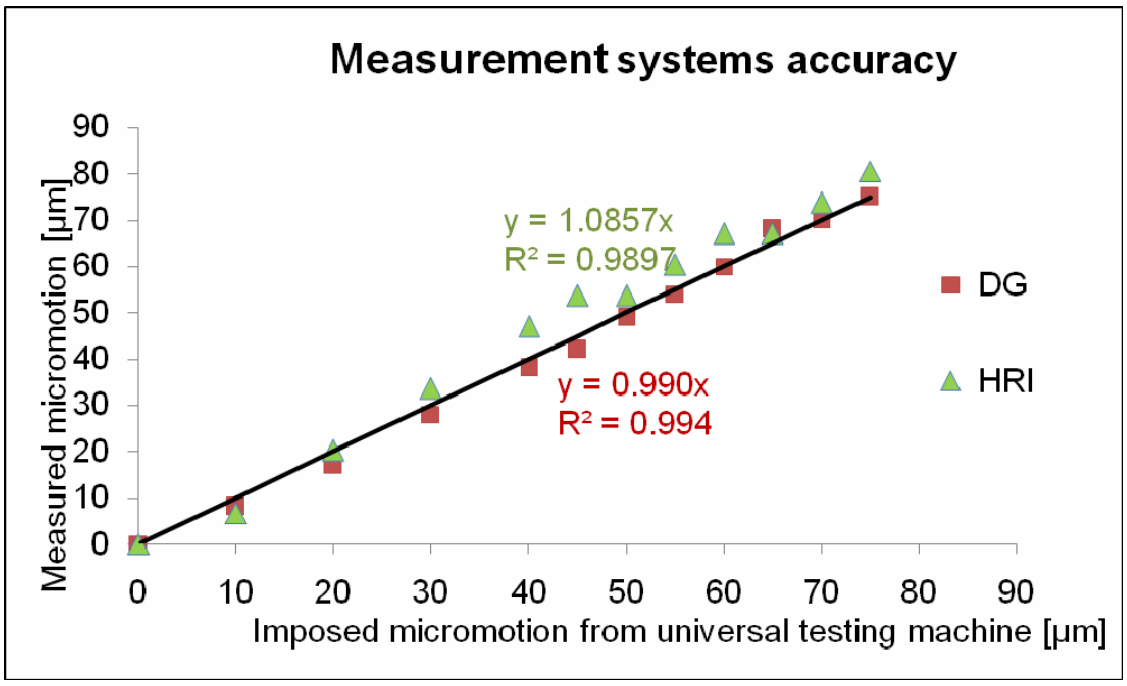

Supplementary Figure 2

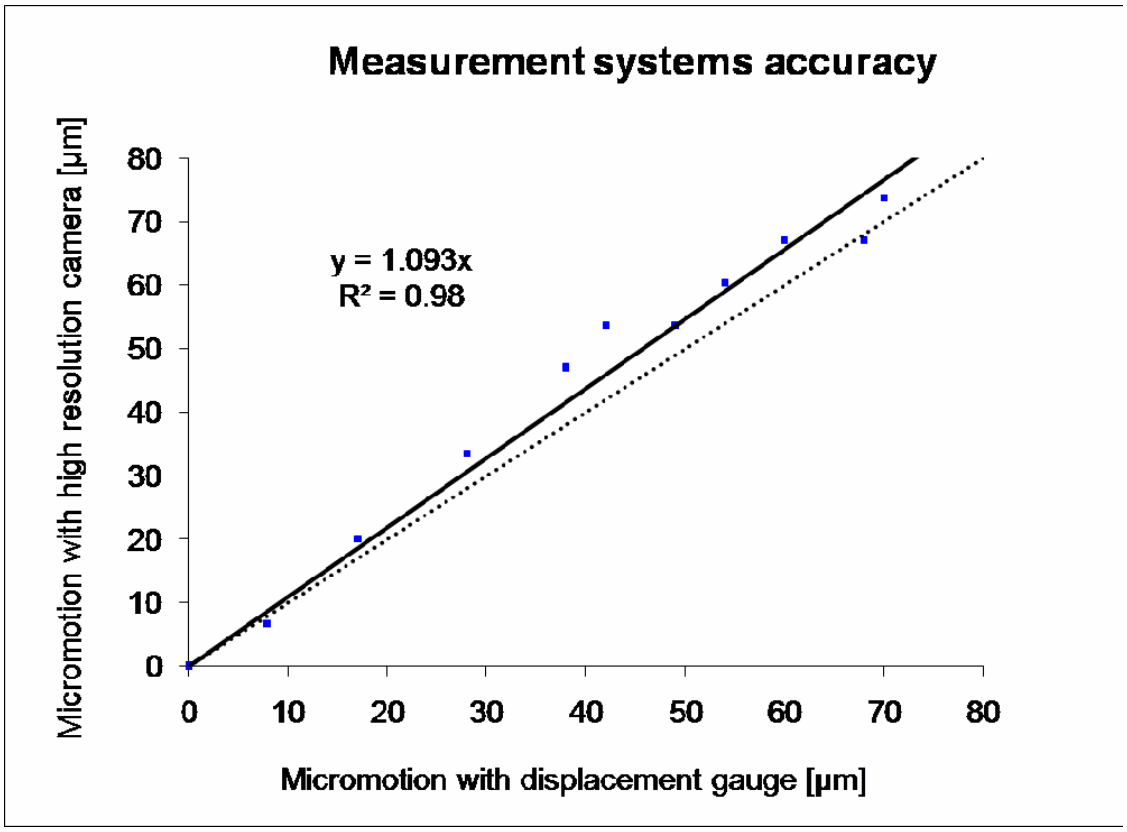

Supplementary Figure 3